Journal of Biomechanics 47 (2014) 1045–1051

Contents lists available at ScienceDirect

Journal of Biomechanics

journal homepage: www.elsevier.com/locate/jbiomech
www.JBiomech.com

Patellar mechanics during simulated kneeling in the natural and implanted knee

Tariq R. Abo-Alhol [a], Clare K. Fitzpatrick [a], Chadd W. Clary [a], Adam J. Cyr [b], Lorin P. Maletsky [b], Peter J. Laz [a], Paul J. Rullkoetter [a,*]

[a] Center for Orthopaedic Biomechanics, University of Denver, 2390 S. York St., Denver, CO 80208, USA
[b] Experimental Joint Biomechanics Laboratory, University of Kansas, Lawrence, KS, USA

ARTICLE INFO

Article history:
Accepted 22 December 2013

Keywords:
Kneeling
Bone strain
Patella
Total knee replacement

ABSTRACT

Kneeling is required during daily living for many patients after total knee replacement (TKR), yet many patients have reported that they cannot kneel due to pain, or avoid kneeling due to discomfort, which critically impacts quality of life and perceived success of the TKR procedure. The objective of this study was to evaluate the effect of component design on patellofemoral (PF) mechanics during a kneeling activity. A computational model to predict natural and implanted PF kinematics and bone strains after kneeling was developed and kinematics were validated with experimental cadaveric studies. PF joint kinematics and patellar bone strains were compared for implants with dome, medialized dome, and anatomic components. Due to the less conforming nature of the designs, change in sagittal plane tilt as a result of kneeling at 90° knee flexion was approximately twice as large for the medialized-dome and dome implants as the natural case or anatomic implant, which may result in additional stretching of the quadriceps. All implanted cases resulted in substantial increases in bone strains compared with the natural knee, but increased strains in different regions. The anatomic patella demonstrated increased strains inferiorly, while the dome and medialized dome showed increases centrally. An understanding of the effect of implant design on patellar mechanics during kneeling may ultimately provide guidance to component designs that reduces the likelihood of knee pain and patellar fracture during kneeling.

1. Introduction

Kneeling after total knee replacement (TKR) has frequently been cited as a limiting activity for patients (Weiss et al., 2002; Noble et al., 2005). Many patients have reported that they cannot kneel due to pain, or avoid kneeling due to discomfort (Shafi et al., 2005; Hassaballa et al., 2002; Nijs et al., 2006; Palmer et al., 2002). For many TKR patients, kneeling is of particular cultural relevance, or is a requirement of their daily activities (praying, gardening). As a result, the ability or lack of ability to kneel without discomfort critically impacts quality of life and perceived success of the TKR procedure (Weiss et al., 2002).

While there are a variety of potential sources of knee pain during kneeling, including scar position (Nijs et al., 2006; Schai et al., 1999), the patellar bone contains numerous pain-sensing mechanoreceptors (Wojtys et al., 1990, McDougall, 2006), and is a likely contributor to anterior knee pain. During kneeling, the ground reaction force on the tibial tuberosity and/or patella causes a posteriorly-directed shear force on the tibia and compressive force on the patella (Incavo et al., 2004; Goldstein et al., 2007). After TKR, patellofemoral conformity, patellar tracking and strains are significantly altered from the native joint. Prior TKR studies have reported bone strains in resected patellae which are substantially higher than the natural knee (McLain and Barger, 1986; Reuben et al., 1991; Lie et al., 2005; Wulff and Incavo, 2000; Fitzpatrick et al., 2011), with resected patellae being more vulnerable to fracture due to sagittal plane bending in deep flexion, particularly in thinner patellae (Reuben et al., 1991). A high flexion, high patellofemoral (PF) contact force activity, such as kneeling, suggests that patients kneeling after TKR may be particularly susceptible to anterior knee pain and patellar fracture (Windsor et al., 1989).

A number of clinical studies have attributed PF complications, including patellar fracture and patellar bone strain, to prosthesis design (Brick and Scott, 1988; Healy et al., 1995; Theiss et al., 1996; Meding et al., 2008; McLain and Barger, 1986). Studies which have investigated the biomechanics of kneeling in TKR knee have predominantly focused on tibiofemoral (TF) kinematics, evaluating in vivo six-degree-of-freedom (6-DOF) kinematics through radiographic techniques (Hanson et al., 2007; Hamai et al., 2008; Incavo et al., 2004; Kanekasu et al., 2004; Coughlin et al., 2007). A number of cadaveric studies have utilized pressure-sensitive

* Corresponding author. Tel.: +1 303 871 3512; fax: +1 303 871 4450.
E-mail address: prullkoe@du.edu (P.J. Rullkoetter).

0021-9290/$ - see front matter © 2014 Elsevier Ltd. All rights reserved.
http://dx.doi.org/10.1016/j.jbiomech.2013.12.040

film to measure PF or TF contact area and pressure in response to kneeling, employing a compressive force, in addition to a quadriceps load, in order to simulate the loads encountered during kneeling (Wilkens et al., 2007; Hofer et al., 2011). Other in vitro studies have measured patellar bone strain using strain gauges attached to the anterior surface of the patella, but have not performed these analyses during a kneeling activity (McLain and Barger, 1986; Wulff and Incavo, 2000; Lie et al., 2005; Reuben et al., 1991). Computational methods have been used to develop high flexion models which have been applied to predict ligament and joint forces but have not been utilized to evaluate knee mechanics under loading conditions which simulate kneeling (Yang et al., 2010; Zelle et al., 2011), or to compare component designs under the high flexion, high PF force loading conditions representative of a kneeling activity.

The objective of the current study was to evaluate the effect of component design on patellar mechanics during a kneeling activity. A computational model to predict PF kinematics and strains after kneeling was developed and kinematics were validated against experimental cadaveric studies. A series of computational models, which included representations of both the native joint and a variety of TKR designs were compared during a simulated kneeling activity. PF joint kinematics and patellar bone strains were compared across multiple specimen-specific finite element (FE) models. An understanding of the effect of implant design on patellar mechanics during kneeling may ultimately provide guidance to component design that reduces the likelihood of knee pain and patellar fracture during kneeling.

2. Materials and methods

2.1. In-vitro cadaveric testing

A series of in vitro tests, designed to simulate a kneeling activity, were performed on four cadaveric knee specimens (male; age: 61.8 ± 13.8 years; height: 1.76 ± 0.08 m; weight: 76.67 ± kg). Each test was initially conducted on the natural knee, with the skin, joint capsule, knee ligaments and musculature intact. Subsequently, testing was performed on a posterior-stabilized (PS) TKR knee system, implanted by an orthopedic surgeon, with two distinct styles of patellar component, a 3 mm medialized dome and an anatomic design, with a consistent femoral and tibial geometry.

The femoral and tibial bone of each specimen was transected approximately 20 cm from the joint line, cemented into aluminum fixtures and mounted in a quasi-static knee rig (QKR) which permitted loading of the quadriceps and contact with a floor to simulate kneeling (Fig. 1). An aluminum clamp was used to rigidly attach the rectus femoris (RF) and vastus intermedius (VI) tendons such that they were actuated along the line-of-action of the femoral shaft. Superior–inferior (S–I) and anterior–posterior (A–P) translation of the simulated ankle position was constrained, while other degrees-of-freedom (DOF) were unconstrained. Knee flexion was achieved through S–I and A–P motion of the simulated hip. The knee was flexed to 90° TF flexion, while maintaining a vertical femur, until the patella made contact with the floor, which was represented by a metal plate with adjustable height. A 90 N load was applied to the quadriceps through free weights attached to the quadriceps tendon, while a contact force of 180 N between the patella and the floor was applied as a result of the weight of the fixtures and femur. The 90 N quadriceps loading counterbalances the weight of the hip sled in the experimental rig and allows the knee flexion angle to remain static.

An Optotrak 3020 (Northern Digital, Waterloo, Ontario) motion analysis system was used to track 6-DOF kinematics of the femur, tibia and patella bones throughout the activity through light emitting diode markers which were rigidly fixed to each bone. A hand-held digitizer was used to collect location data on each TKR component and bone surface relative to its respective local coordinate frame in order to determine component alignment relative to the bone. Magnetic resonance (MR) images (slice thickness of 1 mm; in-plane resolution of 0.234 × 0.234) were obtained for each specimen prior to implantation.

2.2. Finite element model development and kinematic validation

Specimen-specific FE models, which reproduced the in vitro experiment, were developed in Abaqus/Explicit (SIMULIA, Providence, RI) and based on previous models validated for kinematic prediction (Baldwin et al., 2009). Geometry of femoral, tibial and patellar bone and cartilage were segmented from the MR scans using ScanIP software (Simpleware, Exeter, UK). Size-matched TKR component geometry was generated from computer-aided-design surfaces obtained from the manufacturer. Bones and the femoral component were meshed with rigid triangular shell elements, and tibial and patellar components and all articular cartilage surfaces were meshed with deformable, eight-noded hexahedral elements. Implant components were positioned under the guidance of an orthopedic surgeon. The dome was positioned as medial and superior as possible while avoiding overhang. Implanted models also included a layer of bone cement between the patellar component and bone which was meshed with hexahedral elements. For the kinematic validation analyses, bone and the femoral component were modeled as rigid for computational efficiency. Tibial and patellar components were modeled as a nonlinear elastic–plastic material (Halloran et al., 2005a, 2005b), while linear material models were used for bone cement (E=3400 MPa, ν=0.3) and femoral, tibial and patellar articular cartilage (E=12 MPa, ν=0.45). A coefficient of friction of 0.04 was applied between metal–polyethylene articulating surfaces (Halloran et al., 2005a, 2005b). The patellar tendon, RF and vasti tendons were represented by deformable hyperelastic membrane elements with fiber-reinforcement, with uniaxial tension characteristics calibrated to match published experimental measurements (Atkinson et al., 1997; Stäubli et al., 1999). The vasti tendon was separated into five bundles representing the VI, vastus lateralis longus (VLL), vastus lateralis obliquus (VLO), vastus medialis longus (VML) and vastus medialis obliquus (VMO) (Fitzpatrick et al., 2011). Contact was defined between all soft-tissue structures and relevant bone and articular surfaces to allow wrapping in deep flexion. In order to directly reproduce the experimental setup, loading in this case was only applied to the VI bundle of the vasti tendon.

The model was first aligned in the initial position of the kneeling activity based on the measured positions obtained during cadaveric testing. During the kneeling simulation, TF kinematics were fully prescribed based on the experimentally measured kinematics. The patella was kinematically unconstrained, with a 90 N load applied to the RF and VI bundles of the quadriceps, and a compressive load matching the experimental loading condition (180 N) applied to the patella via contact with the floor. 6-DOF PF kinematics were measured in the same manner as the experiment, and compared to the in vitro data.

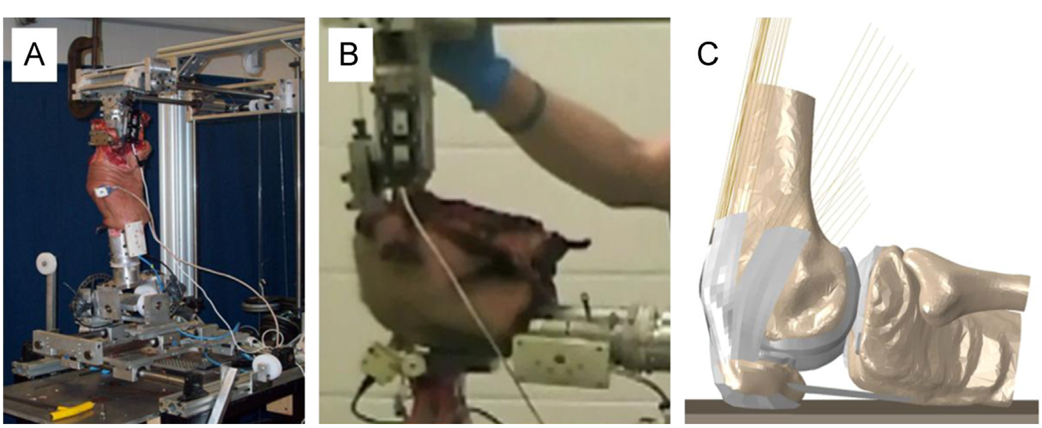

Fig. 1. (A) Knee specimen fixed in the quasi-static knee rig; (B) experimental kneeling simulation in the quasi-static knee rig; and (C) computational simulation of the kneeling experiment.